A Method to Detect and Isolate Brake Rotor Thickness Variation and Corrosion

Hamed Kazemi[1], Xinyu Du[2], and Hossein Sadjadi[3]

[1,3]*General Motors Canadian Technical Centre, Markham, Ontario, L3R 4H8, Canada*
hamed.kazemi@gm.com
hossein.sadjadi@gm.com

[2]*General Motors Global Technical Centre, Warren, Michigan, 48092, USA*
xinyu.du@gm.com

ABSTRACT

Brake rotors are essential parts of the disc brake systems. Brake rotor thickness variation (RTV) and corrosion are among top failure modes for brake rotors, which may lead to brake judder and pulsation, steering wheel oscillations and chassis vibration. To improve customer satisfaction, vehicle serviceability and availability, it is necessary to develop an onboard fault detection and isolation solution. This study presents a methodology to monitor the state-of-health of brake rotor system to reduce costs associated with scheduled inspection for autonomous fleet or corrective maintenance. We converted the vehicle signals from time-domain to angle-domain and determined health indicators to estimate the RTV level of the rotors. Variance, envelope and order analysis of the brake circuit pressure, longitudinal acceleration and wheel speed sensor signals in angle-domain were promising health indicators to differentiate healthy and faulty rotors. A classification model was developed to fuse the health indicators and estimate the state-of-health of the rotors to report the most degraded rotor with corner isolation. Results showed that using this concept we were able to detect failure levels of 20 microns and larger and meet the customer requirement. Robustness analysis showed that the concept is robust to the noise factors of tire type, tire pressure and vehicle weight. The sensitivity analysis showed that the algorithm is sensitive to two of the calibration parameters (i.e., brake pedal position gradient (BPPG) threshold and the filter order used to derive BPPG) used to determine the brake event and enable the algorithm.

https://doi.org/10.36001/IJPHM.2023.v14i1.3377

1. INTRODUCTION

1.1. Background

Brake rotors are critical components of the disc brake system. During braking, the brake hydraulic pressure squeezes a pair of pads against the rotor to generate friction. The pads retard the rotation of the shaft to reduce the rotational speed of the wheel. In this process, the kinetic energy is converted into heat, which is dissipated to the ambient environment.

Brake rotors can deteriorate in performance over their useful life and degrade for several reasons such as: (i) when brakes are applied intensely in quick succession; (ii) disc is worn below the minimum thickness; (iii) pads are excessively worn; and (iv) debris accumulation between pads and disc. These factors normally reduce disc's capacity to dissipate heat and lead to thermal distortion and mechanical deflection (Antanaitis & Robere 2017). Degraded rotors are the main source of "brake judder", where a non-uniform braking torque is applied to the vehicle resulting in brake force fluctuations (de Vries & Wagner 1992, Kao, et al. 2000, Leslie 2004, Kang & Choi 2007). These fluctuations are perceived by driver as vibrations in steering wheel, pulsations in brake pedal, or noise and vibrations from chassis components (Lee & Dinwiddie 1998). Brake judder can further be classified into thermal judder and cold judder. Thermal judder is due to uneven thermal expansion of the disc and occurs during deceleration from high speeds. Cold judder is the most common type of judder and is due to uneven wear or mounting and geometrical irregularities of the disc and may occur at any speed (Lee & Manzie 2016, Bryant, et al. 2008). The frequency of the judder is proportional to the wheel speed. Cold judder is mainly at the first and the second order of the wheel speed frequency and causes lower frequency vibrations in the range of 10Hz to 100Hz, while hot judder causes higher frequency vibrations in the range of 10Hz to 600Hz (Xu & Winner 2015).

Common brake rotor failure modes include RTV – also known as DTV (Disc Thickness Variation), disc lateral runout, and corrosion. RTV refers to an uneven surface of the brake rotor (Rodriguez 2006), which is illustrated in Figure 1. RTV values greater than ~20 micrometers create noticeable brake judder for an experienced driver (de Vries & Wagner 1992).

When RTV fault occurs, a non-uniform braking torque is applied to the vehicle during braking. It is perceived by drivers as brake pulsation or steering wheel vibration. Such a vibration may cause driver's discomfort, or even anxiety about the vehicle safety and quality. Because the variation of the rotor surface is generally about 10 um, which must be measured carefully at multiple locations, the process is slow and costly. Therefore, there is a strong need to develop an automatic prognostic solution for RTV. Autonomous Vehicle (AV) fleet require periodic manual inspection of brake rotors as vehicles are not equipped with instrumentation to provide direct health monitoring. By automating the brake rotor fault detection, there is an opportunity to: (i) reduce the frequency of high-cost operation safety inspection check regarding brake rotors; and (ii) fault isolation allows fast and accurate diagnostics and reduces the time and labor to repair.

Various chassis mechanical components, such as brake rotors, are not equipped with instrumentations to provide direct health monitoring and diagnostics. Therefore, when brake judder is felt by the driver, the thickness of the brake rotor is measured at multiple points to diagnose rotor faults. Significant research has been conducted in prognostics and health management (PHM) with numerous applications of rotary machinery components *e.g.* bearings and gears (Trilla, Dersin and Cabre 2018, Lee, et al. 2014, and Butler, et al. 2012). Building on the existing PHM research (see Nguyen, *et al.* 2019 and Benedettini, *et al.* 2009 for a review), this paper demonstrates new early fault detection capabilities to detect brake rotors thickness variation.

Visual inspection is the most common method for the brake rotor diagnostics, which can be performed during vehicle maintenance. To detect the RTV, the laser measurement technique is one of the effective approaches to directly measure the rotor surface. A diagnostic tool using holographic interferometry is proposed (Beeck & Hentschel, 2000). Holographic interferometry is a type of interferometric approach, which measures the rough surface for static and dynamic displacements of an object. For brake rotor diagnostics, it can be used to generate the contour of the brake rotors surfaces. By observing the images generated, the faulty brake rotors with uneven surfaces can be detected.

The visual inspection cannot be performed onboard, while the vehicle is in operation. To address this issue, some vibration-based approaches are used for brake rotor diagnostics and prognostics. The support vector machine

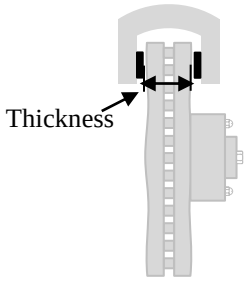

Figure 1. Illustration of Brake Rotor Thickness Variation

based approach is employed (Jegadeeshwaran & Sugumaran, 2015). Vehicle vibration signals for healthy and faulty brake rotors during braking, are collected using piezoelectric type accelerometers. Vehicle condition labels and the statistical features of the accelerometer measurements, such as standard deviation, variance, and kurtosis, are classified by SVM. The faulty brake rotors can then be diagnosed with the trained SVM. The Clonal Selection Classification (CSC) algorithm using the same vibration signals is proposed for rotor diagnostics (Jegadeehwaran & Sugumaran, 2014). The vehicle vibration signals are collected for both good and faulty brake rotors. The statistical feature sets of vibration signals, including standard error, kurtosis, and skewness, are selected, and extracted for classification using an attribute evaluator. The selected feature sets for healthy and faulty brake rotors are then classified using the CSC algorithm.

The brake rotor fault can also be detected using the numerical model and the system dynamics theory (Joe, *et al.* 2008). A linear, lumped, and distributed parameters model is set up to perform the stability analysis. The complex eigenvalues of the model represent the dynamic stability of the brake system. The analysis of eigenvalues can then be applied to detect the instability of the brake system caused by the faulty brake rotors.

In another study, the noise-based approach is employed for rotor fault diagnostics and prognostics (Ertekin & Özkurt, 2019). The noise signals from the healthy and faulty brake rotors during braking are collected and processed using the Wavelet Synchro-squeezed Transform. The noise difference between the healthy and faulty brake rotors can be visualized in the scalogram and verified by a quantitative measure of entropy. As a result, the average entropy value of a faulty brake rotor is higher than the value of a healthy rotor. Accordingly, the entropy value can be used as a fault signature to detect faults.

Although the performance of aforementioned approaches is good for certain test datasets, their robustness under different noise factors or other failure modes is still a concern. Furthermore, some sensors required in these approaches are not available in most vehicles. To address these issues, a novel prognostic approach using existing vehicle signals for brake RTV fault is proposed in this work.

As described in our previous work (Kazemi, *et al*. 2019), three vehicle signals are selected to extract fault signatures based on vibration characteristics.

This research work is preceded by a set of well-defined requirements the brake rotor fault detection algorithm must meet. To preserve the customer ride comfort and provide notifications of a needed service, the brake rotor fault detection algorithm shall detect brake rotor failure before a level an average driver can notice. This failure level is 25 microns of thickness variation. The detection of brake rotor failure shall be done with a high true positive rate while minimizing the false positive rate. Furthermore, the brake rotor fault detection algorithm shall be operational in normal driving conditions and robust to tire type, tire pressure, road conditions and vehicle weight. In addition to the above requirements the brake rotor fault detection algorithm shall only consume vehicle signals from currently available sensors to avoid hardware change or additional cost.

Considering all requirements described above, we propose a novel brake rotor fault detection algorithm. The novelty and contribution, compared to the literature, are summarized as below:

1. Leverage available existing vehicle sensors without the added cost of dedicated instrumentation
2. Provide a framework, including preprocessing and novel HIs to detect common brake rotor faults
3. Provide an estimate of RTV for each wheel through regression and fusion of various health indicators (HIs)
4. Detect fault through correlation of independent sensors: wheel speed sensor (WSS) and brake circuit pressure (BCP)
5. Use the WSS for phase domain transform, and to enable accurate fault isolation to the wheel-level
6. Use the corner correlation HIs to identify brake pressure fluctuations that are associated with rotor degradations

This paper is outlined as follows. Section 2 begins with describing the experimental setup, fault injection procedure, data collection and then details the fault detection and isolation algorithm. It discusses the various building blocks of the algorithm as well as the methodology used to rank various HIs and perform robustness analysis. It also describes our proposed concept to estimate the state of the health of brake rotors. Section 3 presents the results of various analysis obtained from this concept and the performance of this concept is further discussed in section 4. The conclusion is drawn in section 5.

2. MATERIALS AND METHODS

This section provides information on procedures related to fault injection, ground truth definition, measuring the degradation level (RTV), experimental setup, data acquisition, and the various components of the brake rotor fault detection and isolation algorithm used to analyze rotor data and make predictions on the health of the brake rotor system.

2.1. Experimental Setup

2.1.1. Fault Injection

The two most common failure modes were considered: RTV and corrosion. In total, 25 faulty rotors were created. Details of the fault injection procedure can be found in (Kazemi *et al*, 2019). To create faulty rotors, healthy rotors were machined down to generate varying levels of thickness variation (see Figure 2). A “first order” fault profile was injected which involves a uniform thickness variation using a feeler gauge. The first-order RTV profile has one maximum thickness and one minimum thickness. The thickness vs. angle curve approximately resembles a single period of a sinusoid. A “second-order” faulty profile was also injected which has two maxima and two minima, approximately resembling two periods of a sinusoid. When various rotor thickness measurements (about 24 points) were performed across various circumference points, a quasi-sinusoidal profile is produced, and the peak-to-peak amplitude of this profile is reported as RTV (see Figure 3).

(A)

(B)

Figure 2. Brake Rotor Fault Injection (A) machining tool to create the 1st order and 2nd order thickness variation (B) accelerated corrosion exposure

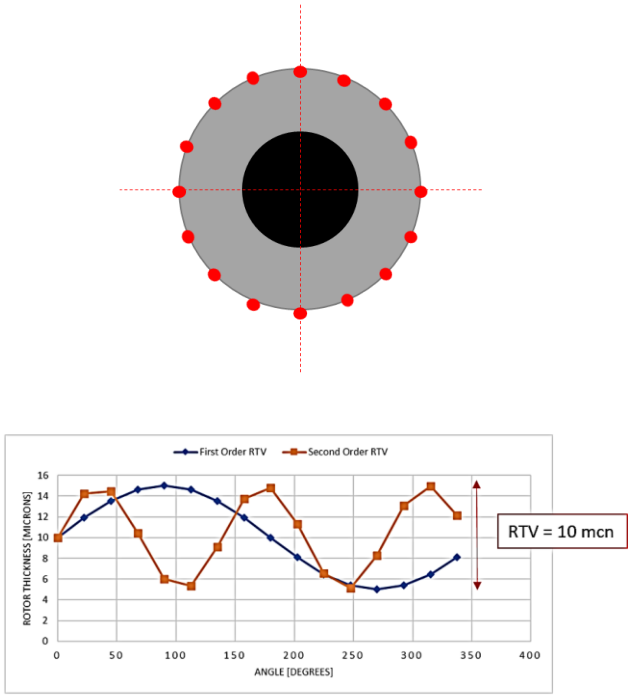

Figure 3. An example of first and second order RTV profile

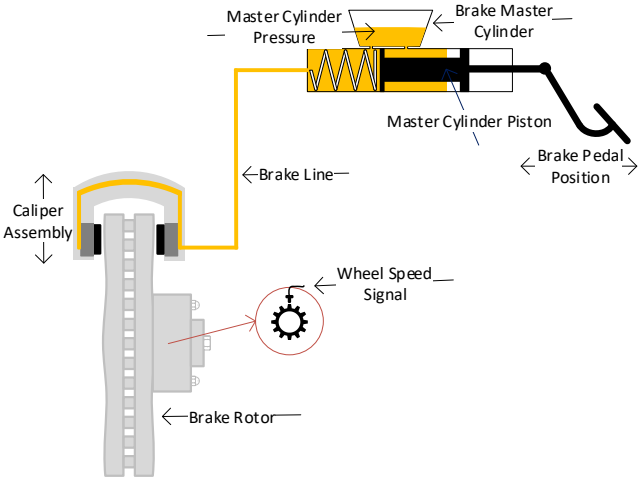

Figure 4. Typical disk brake system illustrating the sensors and signals used to monitor the health of brake rotors

This procedure was repeated five times for each rotor and the median of the calculated RTVs were reported. An accelerated corrosion exposure durability test (salty water spray with certain frequency/duration) was followed to generate the 5-year and 10-year equivalent corroded rotors. A few corroded rotors are shown in Figure 2.

2.1.2. Ground-Truth Definition

The target failure mode for brake rotor prognostics is RTV. This is defined to be the difference between the maximum and minimum thickness of the rotor, typically expressed in microns.

Healthy rotors usually have RTV tolerances less than 5 microns, but up to 10 microns is not uncommon. Note that these values may vary for different vehicles. Between 20 and 50 microns is considered a mild fault where minor acceleration pulses can be noticed and experienced drivers may notice the brake judder at this level, but it will not be overly disruptive. As the RTV levels increase, the steering wheel begins to shake. Above 80 microns is a severe fault, in which the braking experience is uncomfortable and brake judder will be obvious to most passengers.

The RTV profile of a faulty rotor is likely a combination of multiple orders, mostly concentrated on 1st and 2nd order variations. Note that many different rotor profiles may yield the same RTV measurements. That is, the ground truth definition that is used to report the failure level does not distinguish between the profile that is used to generate the fault.

2.1.3. Measurement Setup and Signals

2359 vehicle level road tests were conducted, and data were collected using multiple GM production vehicles. In total, 2359 data sets were generated. 165 test cases were conducted with healthy rotors (*i.e.* RTV = 5-15 µm) and the remainder of the tests were performed with faulty rotors with varying levels of RTV ranging from 21 to 180 µm. Data were collected under the following 8 noise factors:

- Tire type, tire pressure, tire condition, vehicle mass (passenger weight)
- Deceleration rate, brake type, steering maneuver, and driver

Figure 4 shows a simplified diagram of the brake system depicting brake pedal, a hydraulic master cylinder, disc brake assembly, brake lines and hoses. The WSS is also displayed. The master cylinder contains a piston assembly and brake fluid that transfers the hydraulic pressure. The master cylinder is activated by the force applied to the brake pedal by the driver or actuated by a device for the case of an autonomous vehicle. The disk brake assembly includes rotor, caliper, and brake pads. The brake lines and hoses carry the brake fluid to each corner (front left, front right, rear left, rear right), the caliper assembly moves to clamp the spinning disk, and the generated friction force is used to slow or stop the vehicle. Any typical brake system contains sensors to measure the BCP, brake pedal position or boost plunger position. We can also measure the longitudinal acceleration (AX) signal from IMUs as well as wheel speed signal form the WSS available on each wheel. For a faulty brake rotor, we expect that uneven brake rotor surfaces move the caliper piston in and out during

braking, which results in fluid movement in the brake hydraulic system. It is felt all the way in the master cylinder and causes vibration of the BCP. As a result of brake pulsation, we expect to observe vibration in the AX and MCP signals.

The main signals of interest include BCP, AX, Vehicle Speed (VS), WSS, and Brake Pedal Position or its surrogate Boost Plunger Position (BPP). CANalyzer was used to record CAN signals at the rate of 100 Hz. Data were analyzed using MATLAB 2017b.

2.2. Brake Rotor Health Monitoring Algorithm

This section provides details on various components of the brake rotor fault detection and isolation algorithm. First, various function modules of the algorithm are discussed, and then three different concepts are presented on the decision-making logic how various HIs are fused together to make a decision about the health of the algorithm.

The purpose of the brake rotor health monitoring algorithm is to provide early degradation detection of brake rotors that are developing RTV or corrosion. Both identification and isolation of RTV faults are accomplished by performing time and frequency analysis on the brake BCP, AX, and wheel speed signals. More details about the correlation between these signals and rotor fault severity can be found in our previous works (Kazemi, Du, Dixon, & Sadjadi, 2019). Once a fault is detected, this system triggers notifications to make the customer aware of any needed service.

Data are collected both during braking actions as well as during normal driving (non-brake) events. This allows removing background noises during the calculation of HIs and excluding any vibration symptoms caused by other factors (*e.g.* wheel imbalance, rough road). The brake rotor faults are determined if the vibration appears during the braking period but not during the normal driving period.

The block diagram in

Figure 5 shows the core functions and signal flow of the Brake Rotor Health Monitoring function. The algorithm consumes the following vehicle signals:

- Power Mode
- Vehicle Speed
- ABS Control Status
- Stability Control Status
- Traction Control Status
- Boost Pedal Position
- Brake Circuit Pressure
- Longitudinal Acceleration
- Wheel Angular Velocity for each wheel
- Wheel Distance Edge Counter for each wheel

The Brake Rotor Health Monitoring algorithm is divided into sub-functions as summarized below:

2.2.1. Brake Rotor Data Provisioning (DP)

The purpose of this sub-function is to enable and pre-process the vehicle input signals. The Brake Rotor Health Monitoring is enabled when the input signals are valid and meet a set of enabling conditions. The enabled signals are then pre-processed before HI calculation. The Brake Rotor Data Provisioning is divided into three sub-functions as described below:

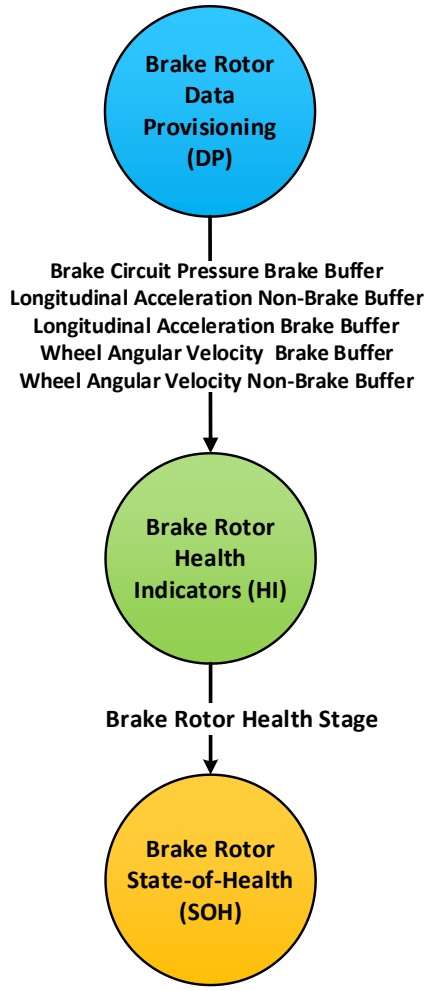

Figure 5. Brake rotor prognostics algorithm has three core function modules: data provisioning, HIs generation and state-of-health generation

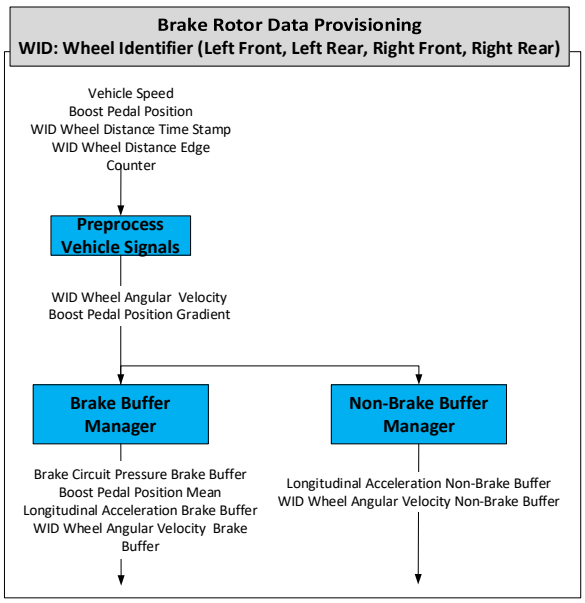

Figure 6. Brake rotor data provisioning (DP) module preprocesses the vehicle signals and manages the brake and non-brake buffers

2.2.1.1 Preprocessing

This sub-function calculates the wheel angular velocity of each wheel from the raw WSS outputs that include the time stamp and the tooth counter. It also computes the gradient of the Boost Pedal Position using a moving average filter.

2.2.1.2 Brake and Non-Brake Buffer Manager

These two sub-functions check the enabling conditions to populate buffers of brake and non-brake signals. All brake and non-brake events are populated in the "phase-domain", with one sample per pulse on the WSS. Therefore, these events all occur over the same number of pulses on the WSS, or the same distance travelled on the ground.

Non-Brake Buffer Enabling Conditions

The enabling conditions to populate non-brake buffers with AX and WS samples include the new value of Wheel Identifier (WID) Wheel Distance Edge Counter is different from the previous value, VS is greater than 10 km/h, Boost Plunger Position Feedback is less than or equal to 5 mm, BCP is less than or equal to 0.02 kPa, and the ABS Control, stability and traction control statuses are inactive. WID refers to the wheel identifier (Left Front (LF), Left Rear (LR), Right Front (RF), Right Rear (RR)). Note that for the vehicle that was tested, the resolution of the wheel speed sensor, brake circuit pressure and longitudinal acceleration were 0.004 rev/s, 0.02 kPa and 0.0625 m/s^2 respectively.

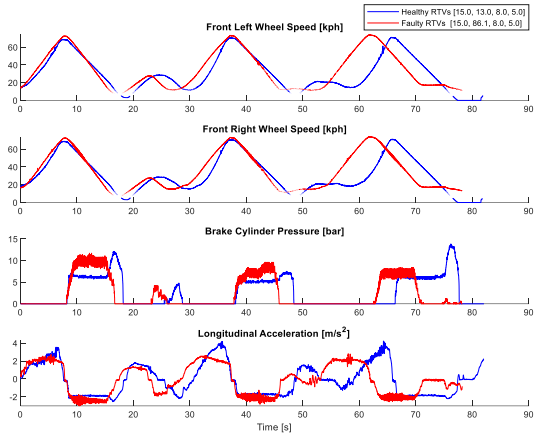

Figure 7. Comparison of a sample healthy and faulty vehicle testing, showing the intuition behind fault signatures.

Brake Buffer Enabling Conditions

The enabling conditions to populate brake buffers with AX, WS, BCP, Boost Pedal Position and Boost Plunger Position are as follows: the new value of WID Wheel Distance Edge Counter is different from the previous value, VS is greater than 10 km/h, VS is less than 256 km/h, Boost Plunger Position Feedback is greater than 6 mm, the absolute value of the Boost Pedal Position Gradient (the derivative of the BPP) is less than 0.005 delta mm, the absolute value of steering wheel angle is less than 5 degree, BCP is greater than 1 kPa, AX is less than 0 m/s^2 and the ABS Control, stability and traction control statuses are inactive.

2.2.2. Brake Rotor Health Indicators

Analyses were performed in both time domain and frequency domain to calculate signatures that are used to detect degradation. These signatures are called HI, which can assess the health of the system and differentiate between a healthy and faulty rotor. Features were selected based on domain expert knowledge, which suggested that the vibration analysis of the MCP, AX signals in time domain (variance) and frequency domain (average order spectrum) can be used to detect abnormalities (Du, et al. 2018). These signals were analyzed during brake and non-brake events. Figure 7 shows a comparison of a vehicle with all healthy rotors and a vehicle with a faulty front right rotor undergoing similar maneuvers, in which the vehicle accelerates to 70 kph and then brakes to 0 kph with approximately constant deceleration at -2 m/s^2. This plot shows some visual information that guided the exploration of possible HIs to yield good results. It can be seen that the faulty vehicle has much higher "judder" or variance in the BCP, AX, and front right wheel speed signal, while the vehicle is braking. Therefore, the objective is to develop a signal processing method that yields in the best possible indicator for quantifying this judder.

The overall function structure of the brake rotor HIs is presented in Figure 8 in which the HIs are calculated from the pre-processed input signals. The calculated HIs are used to speculate the brake rotor State-of-Health (SoH). The data processing for brake rotor HIs is divided into sub-functions as described below:

2.2.2.1 Detrend

The purpose of the detrend sub-function is to remove the linear trend from an input signal. As can be seen in Figure 7, rotor faults result in higher variance in the wheel speed signal from the corner with the degraded rotor. Simply taking the variance of this signal is not a good HI, as the linear trend dominates the variance in this segment of the signal. Applying detrending is quite simple in this case where the brake event is first segmented from the data. A linear line of best fit is first applied to the data, and then simply subtracted as described by Eq. (1) below:

$$\hat{y}(x) = y(x) - (m(x) + b) \tag{1}$$

where m and b are the slope and intercept terms of a linear regression fit to y vs. x. In this case, y represents the signal being detrended (one of BCP, AX, or WS), and x represents the phase domain that the brake buffer signal is mapped to. More details of segmentation and detrending can be found from our previous work (Du *et al*, 2020).

2.2.2.2 Synchronous Averaging

This sub-function calculates the time-synchronous average (TSA) of the main fault detection signals. TSA is a common technique in fault diagnosis of rotating machinery (Lebold, *et al*. 2000). The purpose of TSA is to attenuate components of a signal with a suspected periodic component.

Consider the example of BCP. Given a brake torque command (u), either from the brake pedal or an actuated brake plunger in the AV case, the brake

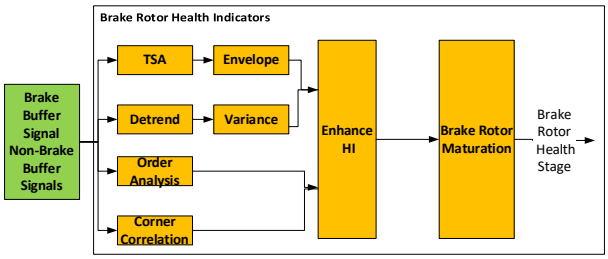

Figure 8. Brake rotor health indicators described the conditions used to define the brake and non-brake events.

control module increases BCP. In the case where the vehicle has a rotor with perfectly uniform thickness (RTV = 0), the BCP signal can be expressed as a function of the control input u and some random disturbance δ:

$$BCP(t) = D(u(t)) + \delta \tag{2}$$

If we assume the rotor is perfectly uniform, we expect this signal to be invariant to rotations of the rotor. However, consider the case where the rotor has a non-zero thickness variation. Given the same control input u, we expect BCP to increase as a thicker portion of the rotor enters the brake pads, forcing the brake pads apart and momentarily increasing the pressure in the hydraulic line. Similarly, we expect BCP to decrease when a thinner portion of the rotor passes between the brake pads, allowing the distance between the pads to contract with no additional force. Therefore, we can model the BCP signal under a faulty rotor as having a periodic component $S(\theta)$ associated with the rotation of each of the vehicle's four wheels, where θ is the rotational phase of the wheel. If we consider each wheel separately, we get the following model of BCP:

$$BCP(t) = D\big(u(t)\big) + S_{FL}\big(\theta_{FL}(t)\big) + S_{FR}\big(\theta_{FR}(t)\big) + S_{RL}\big(\theta_{RL}(t)\big) + S_{RR}\big(\theta_{RR}(t)\big) + \delta \tag{3}$$

However, if we assume that the wheel diameters are equivalent and the vehicle is travelling in a straight line, then the rotational phases of the four wheels are all in synch. We can therefore reduce the above Eq. (3) to Eq. (4)

$$BCP(t) = D\big(u(t)\big) + S\big(\theta(t)\big) + \delta \tag{4}$$

Now, our goal is to estimate S, as we expect this periodic signal to have low amplitude in vehicles with all healthy rotors, and higher amplitudes in vehicles with a faulty rotor. First, we assume that $D(u(t))$ is a linear function, so we can apply linear detrending described in 2.2.2.1 to remove this portion of the signal. This yields the Eq. (5):

$$S\big(\theta(t)\big) + \delta = BCP(t) - (m * BCP(t) + b) \tag{5}$$

The final stage in estimating $S(\theta),\ \theta \in [-\pi, pi]$ is to apply synchronous averaging about the rotational period of the wheel. The synchronous average of a periodic signal S with period T is a signal $TSA(S, \theta)$ with domain $\theta \in [0, T]$ given by Eq. (6):

$$TSA(S, \theta) = \sum_{i=0}^{N-1} S(\theta + iT), \theta \in [0, T] \tag{6}$$

This has the effect of removing high-frequency noise, and only preserving components of the signal that are periodic with period T. In the frequency domain, TSA applies a sort

of "comb" filter that maintains harmonics of the underlying frequency $1/T$. Therefore, we get that

$$S(\theta) = TSA(S + \delta, \theta) = TSA(BCP(t) - (m * BCP(t) + b), \theta(t)) \quad (7)$$

A similar approach is applied to both the AX and WSS signals, in order to estimate any periodic behavior associated with the rotation of the rotors. This calculation can be made simple by first transforming the signal to the phase domain, where each sample is interpolated to be equally spaced by rotational phase of the wheel (and not equally spaced by sampling time, as it is recorded).

2.2.2.3 Envelope

The envelope sub-function is used to quantify a metric of signal "width", under the observation that rotor faults result in more variance and therefore "wider" signals. The envelope of a signal is a smooth curve outlining the upper and lower bounds of the signal. The median envelope difference of the following signals was used as an HI to characterize the degradation level of the rotors:

- Brake Circuit Pressure TSA
- Longitudinal Acceleration TSA
- WID Wheel Angular Velocity Brake Buffer
- WID Wheel Angular Velocity Non-Brake Buffer

as per the logic below:

- Apply a moving-RMS filter that calculates the RMS of each window of size 24 in the signal. This is an estimate of the half-envelope size at each point on the signal.
- Return the median of 2x the moving-RMS filter.

The moving RMS filter is doubled to estimate the difference between the upper and lower envelope.

2.2.2.4 Variance

This sub-function computes the variance of its inputs. The computed variance is used as HI.

2.2.2.5 Order Analysis

The HI sub-functions described so far have all been time-domain indicators. There is also interest in exploring frequency domain indicators, especially since we know that the influence of RTV is periodic with respect to rotation of the wheel. In other words, we are interested in a frequency-domain decomposition of our main fault detection signals, however we want to decompose the signal to sinusoids with units of "samples per revolution", not "samples per second" (as a typical Fourier transform of a uniformly sampled signal would yield). This can be done by order analysis, which is a common approach to quantify vibrations in variable-speed machinery (Brandt 2011). An "order" is a frequency expressed as a multiple of a reference frequency. In the case of brake rotor fault detection, the reference frequency will be the frequency of rotation of the wheel hub assembly.

Traditionally, order-analysis uses two signals recorded from the machine of interest: a target signal x that will be decomposed, and a reference signal r that gives the reference rotational speed for order tracking (typically in RPM). The target signal can be interpolated to the "phase domain," in which samples are equally spaced by rotational phase of the reference shaft and not by time. Taking the discrete Fourier transform of this interpolated signal yields a spectrum in the order domain.

Suppose we apply order analysis to the BCP signal. The average order spectrum indicates that there is a peak at first harmonic (order one). The RMS amplitude at order one is used as a feature or an HI to differentiate between a healthy and faulty rotor. The hypothesis put forward is that for faulty rotors the peak amplitude at order one is larger than healthy rotors. Similar analysis was performed on AX signal and wheel speed.

2.2.2.6 Enhanced Health Indicator

This sub-function applies linear regression to enhance the calculated HIs. A regression to map the HI to health stage is performed using a trained regression model and an additional vehicle signal. The idea is to use mean and variance of vehicle signals (*e.g.*, BPP) for normalization to improve the regression model and reduce the error in estimated RTV value. For example, applying brake pedal at higher rates may result in higher deceleration rate and larger MCP amplitudes which in turn result in observing larger vibration amplitudes. Therefore, there was a need to normalize the HIs (for example, peak to peak amplitude of the vibration) with respect to the BPP. Analysis were performed to determine which vehicle signals are valuable to model. Correlation study presented in Figure 9 revealed that Mean of MCP, AX and BPP are highly correlated (correlation coefficients > 0.95), and therefore only one of the brake-normalizing signals was chosen for any regression model.

2.2.2.7 Brake Rotor Maturation

This sub-function matures the calculated HIs by combining calculations from multiple braking events to remove short-term noises. There are many possible methods of maturation, the most obvious of which are the classic measures of central tendency: median and mean (omitting mode, due to continuity of calculation space). Determining the best performing maturation strategy requires analysis using experimental data. Note, however, that mean maturation has significant advantages, when it comes to memory requirements in an on-board implementation.

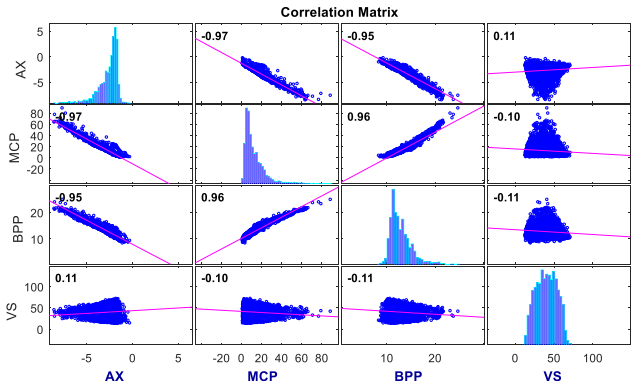

Figure 9. Correlation between vehicle signals during braking events

2.2.3. Rank HIs

A full-factorial set of features from AX, MCP, and 4-corner WS signals and processing techniques (derivative, detrended, variance, kurtosis, skewness, envelope, order analysis, correlation) in both time domain and phase domains were explored. That is, over 2000 HIs were explored and therefore, there is a need to rank these HIs and only select the top performing HIs to differentiate between healthy and faulty rotors. The following criteria were used to rank various HIs: (i) Identifiability: Correlation of the HI with the Ground Truth (GT). An HI with higher correlation to the GT is desired; (ii) Linearity: Deviation from the ideal linear HI. Features with more linear trend rank better than the others; (iii) Compactness: Mean of the standard deviation of the estimated SOHs. HIs that show less variability and dispersion are more appropriate; (iv) Robustness to Noise Factors: An HI is considered robust, when it meets all functional and customer requirements under all operating conditions and its performance is not affected by the variations in the environment, operating conditions or other factors impacting the performance in an undesired way (noise factors). More robust HIs are desired; (v) Monotonicity: To quantify the monotonic trend in HIs as the fault level increases from healthy baseline to the most severe faults. Monotone HIs are preferred as they will likely generalize better to data not used in development; and (vi) Estimation Error: The average relative error between the GT and the prediction obtained from the regression analysis. The lower estimation error indicates more suitable HIs.

HI	Description
Brake Rotor Health Stage	The brake rotor health stage is the best estimate of the maximum RTV of the Four rotors on the vehicle. It is an indicator of the magnitude of fault present.
Brake Circuit Pressure Envelope	The median difference between the upper and lower envelope of detrended BCP data in TSA domain, matured over 15 brake events.
Brake Circuit Pressure Order Analysis (1-4)	Local peak of the order amplitude spectrum of the detrended BCP at orders 1, 1.5, 2, 2.5, 3, 3.5 and 4, matured over 15 brake events.
Brake Circuit Pressure Variance	Variance of the BCP during brake events, matured over 15 brake events.
Boost Pedal Position Mean in Brake Events	Mean of the BPP during brake events, matured over 15 brake events.
Longitudinal Acceleration Envelope	Median of the difference between the upper and lower envelope of detrended AX, matured over 15 brake events.
Longitudinal Acceleration Order Analysis (1-4) in Brake Events	The local peak of the order amplitude spectrum of the detrended AX brake signal at orders 1, 1.5, 2, 2.5, 3, 3.5 and 4, matured over 15 brake events.
Longitudinal Acceleration Order Analysis (1-4) in Non-Brake Events	The local peak of the order amplitude spectrum of the detrended AX non-brake signal at orders 1, 1.5, 2, 2.5, 3, 3.5 and 4, matured over 15 brake events.
WID Wheel Speed Envelope in Brake Events	Envelope of the WID Wheel Angular Velocity during brake events, matured over 15 brake events. WID refers to the wheel identifier (LF, LR, RF, RR).
WID Wheel Speed Envelope in Non-Brake Events	Envelope of the Wheel Angular Velocity during non-brake events, matured over 15 brake events. WID refers to the wheel identifier (LF, LR, RF, RR).
WID Wheel Speed Order Analysis (1-4)	The local peak of the order amplitude spectrum of the WID wheel speed brake signal at orders 1, 1.5, 2, 2.5, 3, 3.5 and 4, matured over 15 brake events.
WID Wheel Speed Variance	This is the variance of the Wheel Angular Velocity, matured over 15 brake events. This interface is used to localize the brake rotor fault.
WID Wheel Speed Enhanced Detection Health Indicator	Enhanced brake rotor HI to estimate the RTV of the four rotors on the vehicle.
Wheel Speed Matured Isolation	This is the matured brake rotor isolation based on Wheel Speed.

Table 1. List of Selected HIs for algorithm development

2.2.4. Selected HIs

Table 1 introduces the top performing HIs that were calculated to differentiate between a healthy and faulty rotor and predict the failure level (RTV).

2.2.5. Brake Rotor State-of-Health Concepts

The goal of the brake rotor SoH function is to collect the system's HIs to provide an estimate of the system's SoH. We investigated various concepts to fuse the HIs that are summarized in. More details are provided below for the most degraded rotor detection and isolation Concept. Other concepts are not explained in this paper.

- **Most Degraded Rotor Detection and Isolation**

The goal of this concept is to detect and isolate the most degraded brake rotor across four wheels. This concept consists of two classifiers as depicted in Figure 10 and described below:

– **Brake Rotor Fault Detection**

This function performs the healthy vs. faulty classification to determine whether there is a faulty brake rotor present in the vehicle. If the matured enhanced BCP envelope HI or the matured enhanced WID envelope HI is greater than the specified threshold, the brake system is labeled as faulty.

– **Brake Rotor Fault Isolation**

The brake rotor fault isolation identifies which wheel is the most likely source of the fault as per the following logic: 1) For each wheel LF, RF, LR, RR, determine the number of instances in the past *11* brake events in which the wheel had the maximum value of *WID Wheel Speed Variance* out of the four wheels. 2) Select the wheel with the highest count of the maximum value instances. 3) If the highest count is at least 4, then identify this wheel as the isolated source of the fault. Otherwise, issue "no decision" and do not isolate the wheel.

Concept	Performance	Complexity
Most Degraded Rotor Detection and Isolation	Detects the most degraded rotor with corner isolation	Average – uses two classifiers
Wheel-level RTV Estimation	Reports estimated RTV of all four corners	Highest – uses regression models for each wheel
Axle-level RTV Estimation and Axle-Isolation	Detects the most degraded rotor with axle isolation	High – uses a mix of classification and regression model

Table 2. Concepts explored to determine the brake rotor state-of-health

2.2.6. Robustness Analysis

Robustness of the algorithm to three noise factors of tire type, tire pressure and passenger weight (gross vehicle mass) were investigated. For each noise factor, two levels were considered for comparison. That is, summer tires vs. winter tires, tire pressure at 30 psi vs. 47 psi and passenger weight of 145 kg vs 290 kg. SOH estimates across two levels of each noise factor were compared using paired *t*-test and significance levels were considered at $p < 0.05$. Note that a subset of data from each noise factor was chosen that included similar number of brake events and same failure modes. Wilcoxon signed rank test was used instead of the paired-*t* test if the normal distribution assumption is violated. Robustness analysis for the binary decisions derived from the Most Degraded Detection concept was performed using Binomial tests to test the hypothesis that the two datasets have the same underlying probability of correct classification.

3. RESULTS

3.1. Representative Signals During Brake and Non-Brake Events

Figure 11 shows an example of MCP, AX, BPP and WS signals for a vehicle with all four healthy rotors (rotor IDs # & 12) (see B) and a vehicle with 1st order faulty (rotor ID #26) RTVs (see C) during braking events. BPP signal shows that there were multiple braking actions in which vehicle decelerated form 60km/h to <10 km/h. Visual inspection

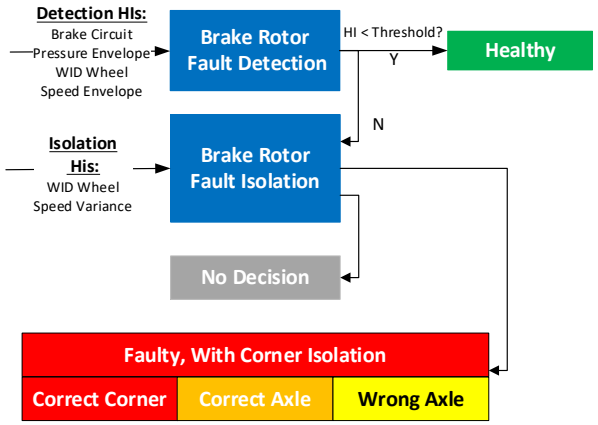

Figure 10. Summary of health indicators used and decision-making logic

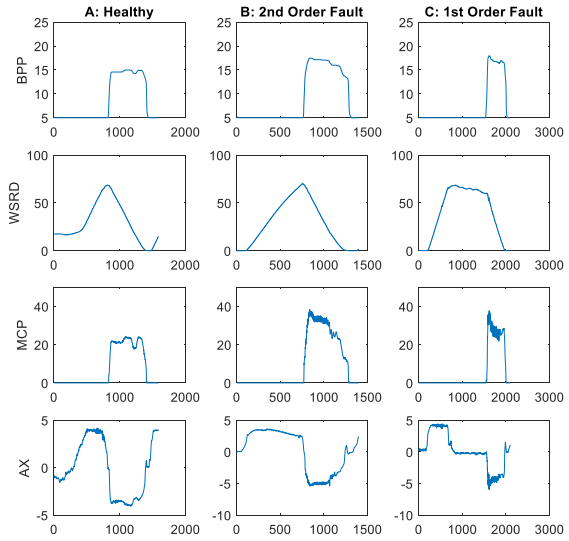

Figure 11. Representative Raw Signals for a vehicle with healthy rotors (A), 2nd order faulty RTV (B) and 1st order faulty rotors (C)

reveals that the variation in both MCP and AX signals are larger for the faulty rotors compared to the healthy one. This was a consistent behavior across all RTV levels and for both 1st order and 2nd order profiles. As RTV increased, the vibration and variance of both MCP and AX signals were also increased during braking actions.

3.2. Representative HIs

Figure 12-A shows an example of an average order spectrum of MCP for 5 Y.E corroded rotor with RTVs of 45 µm at front left, 23 µm rear left, 45 µm front right and 26 µm at rear left corner. Significant difference in the peaks and also the area under the order spectrum can be seen compared to the healthy rotors shown in Figure 12-B. Figure 13 shows an example of average order spectrum of MCP signal and Ax signal for the first and second order RTV fault.

3.3. Ranking HIs

Figure 14 shows the overall results of applying ranking HI framework to the 264 sample of HIs. The top performing HI was determined to be the total peak value of the average order spectrum of the detrended MCP. Results showed that the peak of the average order spectrum of detrended MCP signal outperformed other HIs by having a higher correlation to the GT, less variability, with higher monotonic trend and lower estimation error. The normalized performance metrics for identifiability, linearity, monotonicity, variability, and relative estimation error is shown for all the HIs. It is sorted to display the features in the order of importance based on the average of the metrics used to rank HIs.

3.4. Most Degraded Rotor Detection and Isolation Concept Performance

Figure 15 shows the performance of the most degraded rotor detection with corner isolation concept. The horizontal bars in Figure 15 (A & B) indicate the correct classification rate for each rotor. The y-axis legend corresponds to each rotor and the RTV values in brackets correspond to the four corners of the vehicle (Front Left, Rear Left, Rear Right, Front Right) respectively. The confusion matrix for the corner isolation is also presented in Figure 15 (C). As mentioned, data were collected with several noise factors and in this study, we investigated the robustness of the developed algorithm to the following noise factors: Tire type, tire pressure, and vehicle mass (passenger weight). This concept passed the robustness tests using Binomial tests.

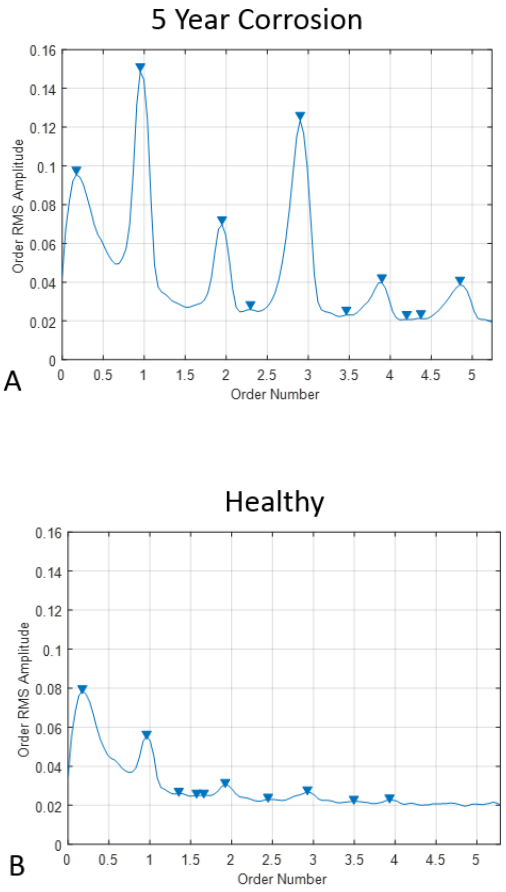

Figure 12. An example of average order spectrum for a faulty rotor (left) vs. healthy rotor (right)

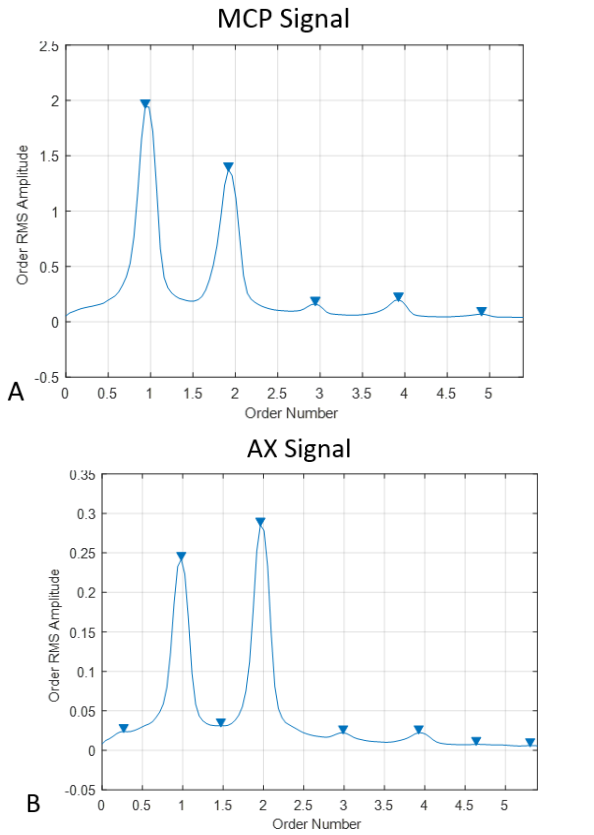

Figure 13. An example of average order spectrum of MCP signal (A) and AX signal (B) for a blended 1st and 2nd order fault (Rotor IDs 23 and 24)

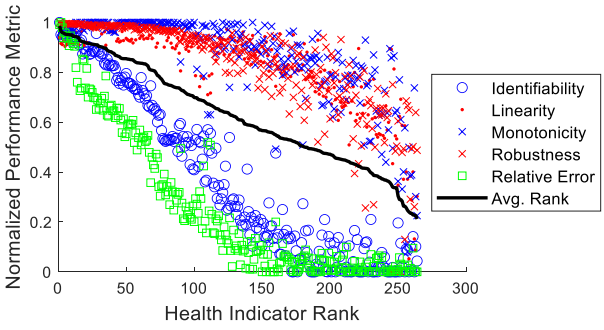

Figure 14. Applying rank HI framework to the developed HIs

3.5. Time to Detection

To find out how often the enabling conditions will be met in normal daily use conditions, a separate analysis was performed by stitched together 5 hours (250 km) of city driving data from 29 different test cases, four different vehicles, by naturally driving around Oshawa/Durham region in Ontario, Canada. By applying the enabling conditions to the distribution of Braking Events in natural driving we observed around 570 braking events in 5 hours of city driving data. That is, on average every 30 seconds we had a braking event. Our algorithm uses 11 braking events to make a decision, and the results show that the mean and median of the time to decision are 4.35 and 6.8 min respectively.

3.6. Sensitivity Analysis

The enabling condition parameters set for the maximum boost plunger position gradient (BPPG) and the filter order applied to the BPPG calculation are the two most significant parameters that require more attention to tune. The brake rotor algorithm is only enabled whenever the moving average filtered boost plunger position (BBP) gradient is less than *MaxBPP_Grad*. If the boost plunger position is changing, then MCP changes as well. Any pressure changes caused by rotor faults are dominated by pressure changes from changing plunger position. Therefore, small values for *MaxBPP_Grad* typically yield better results. Example of how brake buffers are being filled when small value is used for Boost Plunger Position Gradient is shown in Figure 16. Also, *FilterDerivativeOrder* controls the filter applied to the gradient calculation. Larger values yield smoother enabling but introduce a delay when if BPP changes rapidly.

In addition, the number of brake events to combine to mature each HI affects the performance. Longer maturation window size usually leads to improved performance at the cost of increasing time to detection. Default value is 11. If maturation window size is set to a small value, the performance will be significantly impacted. Minimum number of instances of a wheel having the maximum isolation HI to return a matured isolation of the wheel. Default value is 4. Smaller values lead to increased incorrect decisions and higher values increase the number of no decisions outputted.

4. CONCLUSIONS

The purpose of this research is to develop a comprehensive fault detection, isolation and prognosis methodology for brake rotors based on our preliminary work (Du et al, 2020). This study presented a methodology to monitor the state-of-health of brake rotor system to reduce costs associated with scheduled inspection or corrective maintenance. Time and phase domain signal processing were performed to generate several features to estimate the vibration levels caused by a degraded rotor and a ranking framework was introduced to select the top performing HIs. Variance, Envelope and Order Analysis of the MCP, AX and WSS signals were promising HIs to differentiate between healthy and faulty rotors. Three concepts were developed to fuse the HIs and estimate the state-of-health of the rotors by: (i) reporting the

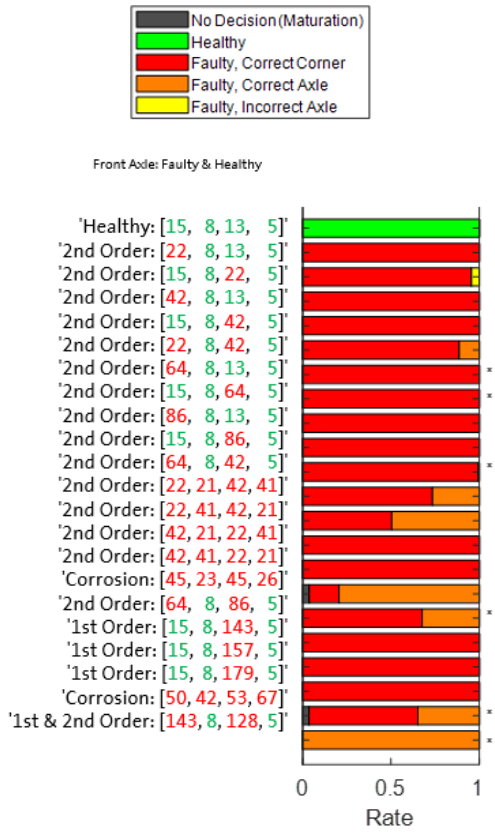

(A)

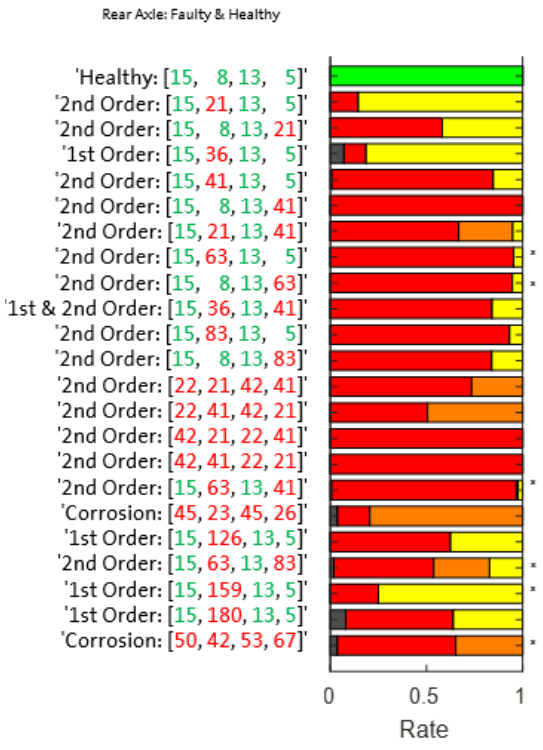

(B)

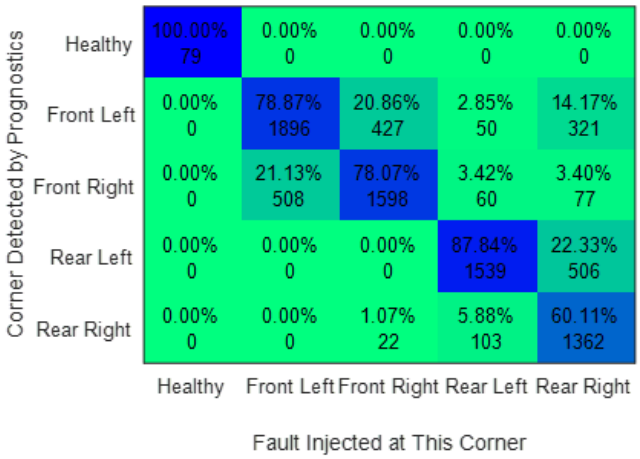

(C)

Figure 15. Most degraded rotor detection and isolation concept performance - test data, (A) & (B) Breakdown of the performance for front and rear rotors, (C) Overall confusion matrix

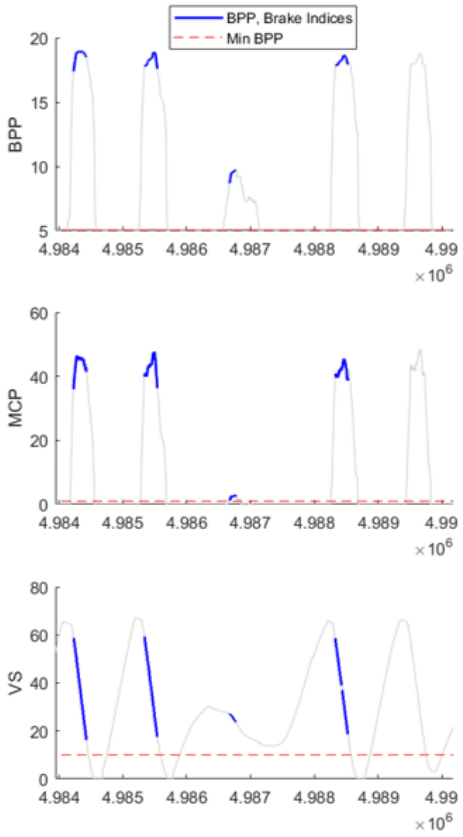

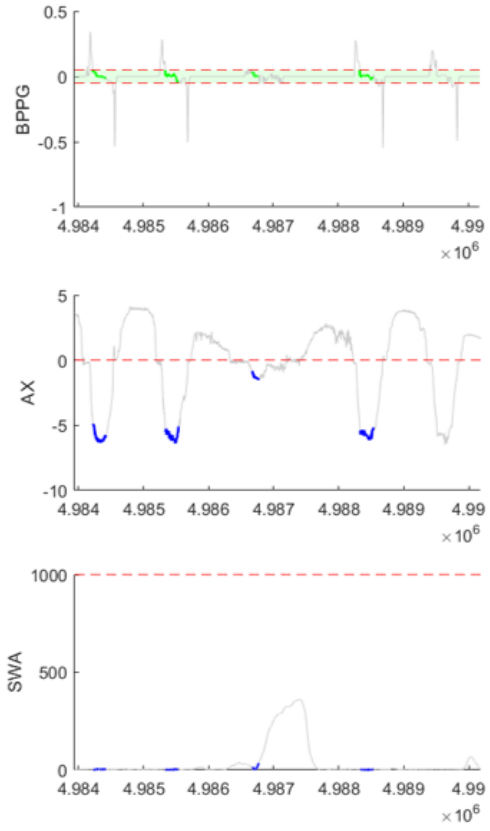

Figure 16. Example of how brake buffers are being filled when small value is used for Boost Plunger Position Gradient. Blue lines show where the algorithm is enabled. When BPPG threshold is small, the large jumps in MCP are removed from the enabled segments. This greatly improves fault detection performance, at the cost of time to detection.

most degraded rotor with corner isolation; (ii) estimate the RTV of each wheel; and (iii) report the RTV of the axle with most degraded rotor. Results showed that using the most degraded rotor detection with corner isolation concept we were able to detect failure levels of 20 microns and larger and meet the customer requirement. Even though the performance of our proposed algorithms is great for the existing test datasets, the performance for the large-scale fleet of vehicles is not obtained yet. Considering the variety of driving environment or maneuvers, and the potential long tail of corner cases, in the next step, we will leverage our telematics platform to collect the vehicle signals, algorithm performance data, and warranty data. The self-evolving or adaptive algorithms will be developed in the future to automatically improve/calibrate the algorithms. The remaining useful life estimation of the brake rotors is also our next focus.

ACKNOWLEDGEMENT

We thank Graeme Garner and Samba Drame for their contributions to this project. We also thank the Advanced Vehicle Prognostics team in General Motors for donating their time and assist with driving the test vehicles and data collection.

NOMENCLATURE

RTV	rotor thickness variation
DTV	disk thickness variation
HI	health indicator
SOH	state of health
WS	wheel speed
WSS	wheel speed sensor
BCP	brake circuit pressure
AX	longitudinal acceleration
DP	data provisioning
WID	wheel identifier
TSA	time-synchronous average
MCP	master cylinder pressure
BPP	brake pedal position
BPPG	brake pedal position gradient
GT	ground truth

REFERENCES

Antanaitis, D. B., & Robere, M. (2017). Brake System Performance at Higher Mileage. SAE International Journal of Passenger Cars-Mechanical Systems, 10(2017-01-2502), 748-763.

Bryant, D., Fieldhouse, J., Crampton, A., Talbot, C., & Layfield, J. (2008). Thermal brake judder investigations using a high speed dynamometer (No. 2008-01-0818). SAE Technical Paper.

Butler, Shane, Frank O'Connor, Des Farren, and John V Ringwood. 2012. "A feasibility study into prognostics for the main bearing of a wind turbine." *2012 IEEE International Conference on Control Applications* 1092-1097.

Brandt, Anders. Noise and Vibration Analysis: Signal Analysis and Experimental Procedures. Chichester, UK: John Wiley and Sons, 2011.

Benedettini, O., Baines, T. S., Lightfoot, H. W., & Greenough, R. M. (2009). State-of-the-art in integrated vehicle health management. Proceedings of the Institution of Mechanical Engineers, Part G: Journal of Aerospace Engineering, 223(2), 157-170.

Beeck, M. A., & Hentschel, W. (2000). Laser metrology — a diagnostic tool in automotive development processes. Optics and Lasers in Engineering, 34(2), 101-120.

de Vries, A., & Wagner, M. (1992). The brake judder phenomenon (No. 920554). SAE Technical Paper.

Du, Xinyu, Dongyi Zhou, Mutasim Salman, Kevin Cansiani, Xiaoyu Huang, and Wen-Chiao Lin. 2018. "detection of a friction brake fault". Patent Granted.

Du, X., Mai, L., Kazemi, H., & Sadjadi, H. (2020, November). Fault Detection and Isolation for Brake Rotor Thickness Variation. In Annual Conference of the PHM Society (Vol. 12, No. 1, pp. 8-8).

Ertekin, Z., & Özkurt, N. (2019). Noise analysis of air disc brake systems using wavelet synchro squeezed transform. Celal Bayar Üniversitesi Fen Bilimleri Dergisi, 15(4), 409-414.

Jegadeehwaran, R., & Sugumaran, V. (2014). Brake fault diagnosis using Clonal Selection Classification Algorithm (CSCA) – A statistical learning approach. Engineering Science and Technology, 18.

Jegadeehwaran, R., & Sugumaran, V. (2015). Fault diagnosis of automobile hydraulic brake system using statistical features and support vector machines. Mechanical Systems and Siganl Processing, 52-53, 436-446.

Joe, Y. -G., Cha, B. -G., Sim, H. -J., Lee, H. -J., & Oh, J. -E. (2008). Analysis of disc brake instability due to friction-induced vibration using a distributed parameter model. International Journal of Automotive Technology, 9, 161-171.

Jalali Milad, Garner Graeme, Sadjadi Hossein, Kazemi Hamed, System and Method for Assessing Health of Brake Rotors, Patent Filed (2021)

Kang, J., & Choi, S. (2007). Brake dynamometer model predicting brake torque variation due to disc thickness variation. Proceedings of the Institution of Mechanical Engineers, Part D: Journal of Automobile Engineering, 221(1), 49-55.

Kao, T. K., Richmond, J. W., & Douarre, A. (2000). Brake disc hot spotting and thermal judder: an experimental and finite element study. International Journal of Vehicle Design, 23(3-4), 276-296.

Kazemi, H., Du, X., Drame, S., Dixon, R., & Sadjadi, H. (2019, September). A prognostics model to predict brake rotor thickness variation. In Annual Conference of the PHM Society (Vol. 11, No. 1).

Lee, Chih Feng, and Chris Manzie. 2016. "Active brake judder attenuation using an electromechanical brake-by-wire system." *IEEE/ASME transactions on mechatronics* 2964-2976.

Lee, Jay, Fangji Wu, Wenyu Zhao, Masoud Ghaffari, Linxia Liao, and David Siegel. 2014. "Prognostics and health management design for rotary machinery systems—Reviews, methodology and applications." *Mechanical systems and signal processing* 314-334.

Lebold, M., McClintic, K., Campbell, R., Byington, C., & Maynard, K. (2000, May). Review of vibration analysis methods for gearbox diagnostics and prognostics. In Proceedings of the 54th meeting of the society for machinery failure prevention technology (Vol. 634, p. 16). Virginia Beach, VA.

Leslie, A. C. (2004). Mathematical model of brake caliper to determine brake torque variation associated with disc thickness variation (DTV) input. SAE transactions, 1193-1203.

Lee, K., & Dinwiddie, R. B. (1998). Conditions of frictional contact in disk brakes and their effects on brake judder. SAE transactions, 1077-1086.

Nguyen, D. V., Kefalas, M., Yang, K., Apostolidis, A., Olhofer, M., Limmer, S., & Bäck, T. H. W. (2019). A review: Prognostics and health management in automotive and aerospace. International Journal of Prognostics and Health Management, 10(2), 35.

Peng, Y., Wong, C., Wang, Z., Wan, F., Vai, M. I., Mak, P. U., . . . Rosa, A. C. (2019). Fatigue evaluation using multi-scale entropy of EEG in SSVEP-Based BCI. IEEE Access, 108200-108210.

Rodriguez, A. 2006. "Experimental analysis of disc thickness variation development in motor vehicle brakes." *Thesis.*

Trilla, Alexandre, Pierre Dersin, and Xavier Cabre. 2018. "Estimating the Uncertainty of Brake Pad Prognostics for High-speed Rail with a Neural Network Feature Ensemble." *PHM Society Conference.*

Xu, Xinfu, and Hermann Winner. 2015. "Experimental investigation of hot judder characteristics in passenger cars." EuroBrake 2015 1-12.